INTEGRAL

Science Operations Centre

Announcement of Opportunity for Observing Proposals (AO-4)

JEM-X Observer's Manual

INT/SDG/05-0248/Dc

Issue 4.1

4 April 2006

Prepared by P. Kretschmar

Authorised by A.N. Parmar

Based on inputs from the JEM-X team, DSRI Copenhagen (PI: N. Lund)

Table of Contents

1 Introduction

The Joint European Monitor for X-rays (JEM-X) on-board INTEGRAL fulfils three roles:

It provides complementary data at lower energies for the studies of the gamma-ray sources observed by the two main instruments, IBIS and SPI. Normally any gamma-ray source bright enough to be detected by the main instruments will also be bright enough to be rapidly identified with JEM-X. Note, however, that the field of view of JEM-X is significantly smaller than those of IBIS and SPI. Flux changes or spectral variability at the lower energies may provide important elements for the interpretation of the gamma-ray data. In addition, JEM-X has a higher spatial resolution than the γ-ray instruments. This helps with the identification of sources in crowded fields.

During the recurrent scans along the galactic plane JEM-X provides rapid alerts for the emergence of new transients or unusual activity in known sources. These sources may be unobservable by the other instruments on INTEGRAL.

Finally, JEM-X can deliver independent scientific results concerning sources with soft spectra, serendipitously detected in the field of view (FOV) during the normal observations.

JEM-X operates simultaneously with the main gamma-ray instruments IBIS and SPI. It is based on the same principle as the two gamma-ray instruments on INTEGRAL: sky imaging using a coded aperture mask. The performance of JEM-X is summarised in Table 1.

Table 1: parameters and performance of the JEM-X1 unit

Parameter	**In-orbit value**
Active mask diameter	535 mm
Active detector diameter	250 mm
Distance from mask to detector entrance window	3401 mm
Energy range	3-35 keV
Energy resolution (FWHM)	$\Delta E/E = 0.40 \times [(1/E \text{ keV})+(1/120 \text{ keV})]^{1/2}$
Angular resolution (FWHM)	3′
Field of view (diameter)	4.8° Fully illuminated 7.5° Half response[1] 13.2° Zero response
Relative point source location error	1 ′ (90% confidence radius for a 15σ isolated source)
Continuum sensitivity **for a single JEM-X unit** (isolated source on-axis)	1.2×10^{-4} ph cm^{-2} s^{-1}keV^{-1}@ 6 keV 1.0×10^{-4} ph cm^{-2} s^{-1}keV^{-1}@ 30 keV for a 3σ cont. detection in 10^5 s, dE = 0.5E
Narrow line sensitivity **for a single JEM-X unit** (isolated source on-axis)	1.6×10^{-4} ph cm^{-2} s^{-1}@ 6 keV 1.3×10^{-4} ph cm^{-2} s^{-1}@ 20 keV for a 3σ line detection in a 10^5 s observation
Timing resolution	122 μs (relative timing) ≈1 ms (absolute timing)

[1] At this angle the sensitivity is reduced by a factor 2 relative to the on-axis sensitivity. In practice, the transmission of the collimator beyond an off-axis angle of 5° is so low that only the very brightest sources can be observed at larger angles

2 Description of the instrument

2.1 The overall design and status

JEM-X consists of two identical coded-aperture mask telescopes co-aligned with the other instruments on INTEGRAL. In the current configuration the JEM-X "1" unit is operating while JEM-X "2" is dormant. The photon detection system of JEM-X consists of high-pressure imaging Microstrip Gas Chambers located at a distance of 3.4 m from each coded mask. Figure 1 shows a schematic diagram of one JEM-X unit. A single JEM-X unit comprises three major subsystems: the detector, the associated electronics and the coded mask.

At the end of the Instrument Performance Verification phase, it was decided to operate only one JEM-X unit at at a time. The switch-off of one of the units was decided after a gradual loss in sensitivity had been observed in both JEM-X units, due to the erosion of the microstrip anodes inside the detector. By lowering the operating voltage, and thereby the gain of the detectors, the anode damage rate has now been reduced to a level where the survival rate of the detectors seems to be assured for the extended mission phase. If in the future both units are to be switched on together again, the total sensitivity will increase by approximately a factor $\sqrt{2}$, however at the time of writing of this document such a change is not being considered

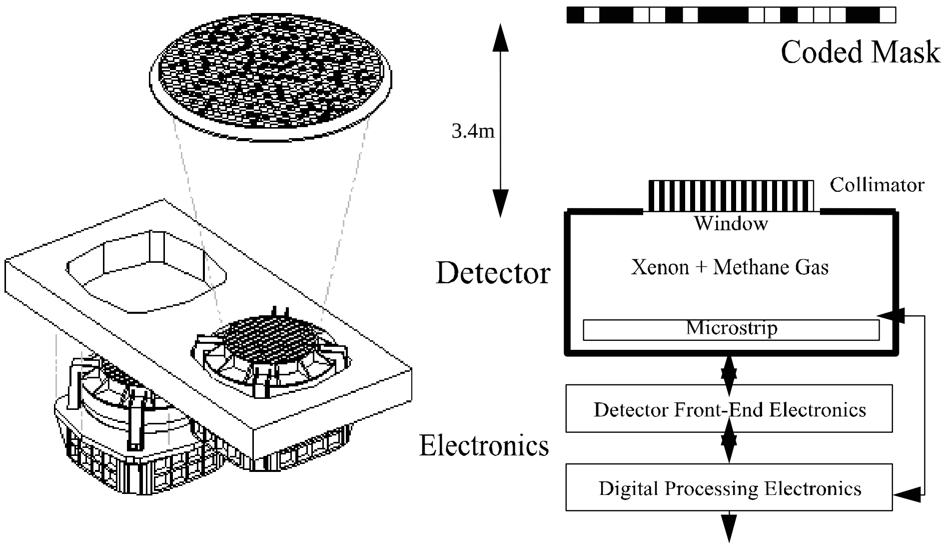

Figure 1: Left: overall design of JEM-X, showing the two units, with only one of the two coded masks. Right: functional diagram of one unit.

2.2 The detector

The JEM-X detector is a microstrip gas chamber with a sensitive geometric area of ~500 cm^2 per unit. The gas filling is a mixture of xenon (90%) and methane (10%) at 1.5 bar pressure. The incoming photons are absorbed in the xenon gas by photo-electric absorption and the resulting ionisation cloud is then amplified in an "avalanche" of ionisations by the strong electric field near the microstrip anodes. Significant electric charge is picked up on the strip as an electric impulse. The position of the electron avalanche in the direction perpendicular to the strip pattern is measured from the centroid of the avalanche charge. The orthogonal coordinate of an event is obtained from a set of electrodes deposited on the rear surface.

The X-ray window of the detector is composed of a thin (250 μm) beryllium foil which is impermeable to the detector gas but allows a good transmission of low-energy X-rays.

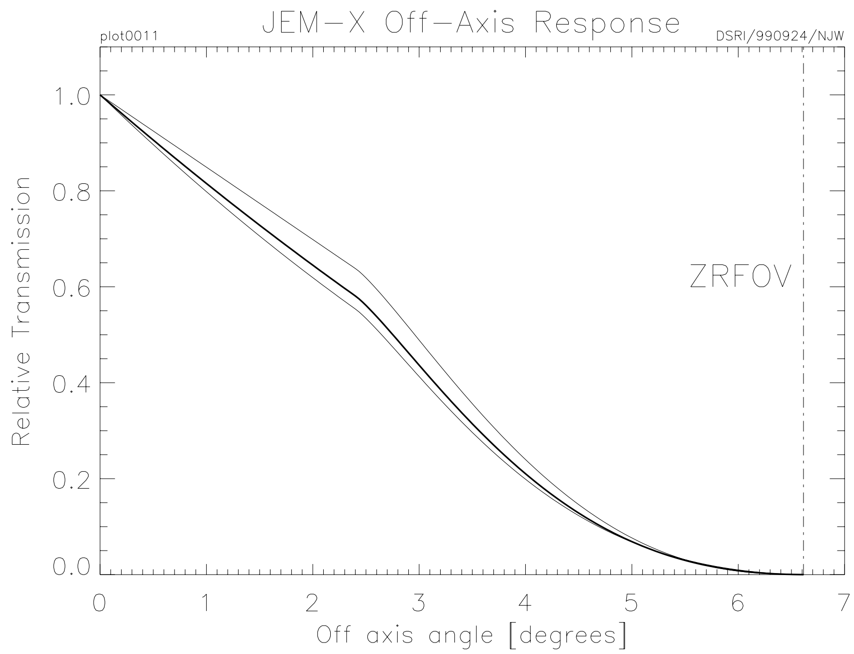

Figure 2: Off-axis response of JEM-X below 50 keV. The middle curve shows the average transmission through the collimator including all azimuth angles.

A collimator structure with square-shaped cells is placed on top of the detector entrance window. It gives support to the window against the internal pressure and, at the same time, limits and defines the field of view of the detector. It has an 85% on-axis transparency. The collimator is important for reducing the count rate caused by the cosmic diffuse X-ray background. However, the presence of the collimator also means that sources near the edge of the field of view will be attenuated with respect to on-axis sources (see Fig. 2). The materials for the collimator (molybdenum, copper, aluminium) have been selected in order to minimise the detector background caused by K fluorescence.

Four radioactive sources are embedded in each detector collimator in order to calibrate the energy response of the JEM-X detectors in orbit. Each source illuminates a well defined spot on the microstrip plate. The gain of the detector gas is monitored continuously with the help of these sources. Figure 3 shows the collimator layout and the locations of the calibration sources.

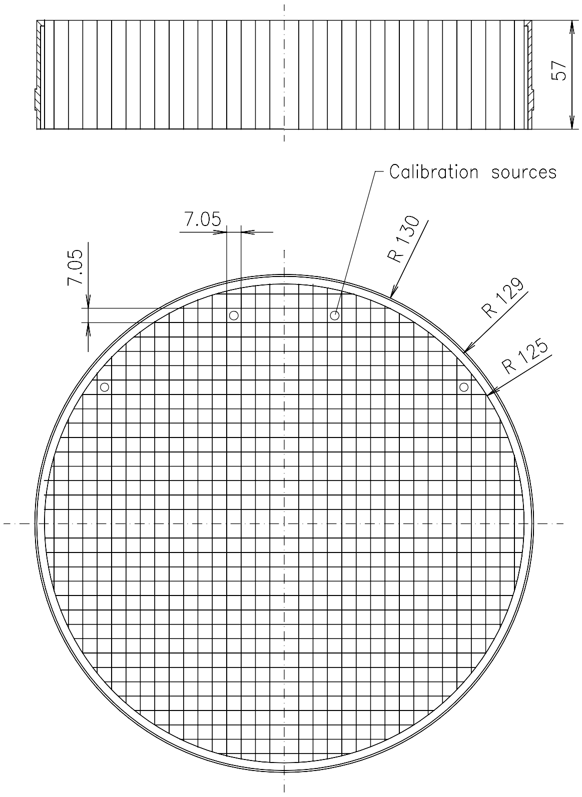

Figure 3: Collimator layout. In this diagram the 4 calibration sources are situated on the upper side. The dimensions are in mm, i.e. collimator length = 57 mm, radius = 130 mm

2.3 The coded mask

The mask is based on a Hexagonal Uniformly Redundant Array (HURA). For JEM-X a pattern composed of 22501 elements with only 25% open area has been chosen. The 25% transparency mask actually achieves better sensitivity than a 50% mask, particularly in complex fields with many sources, or in fields where weak sources should be studied in the presence of a strong source. A mask with lower transparency also has the advantage of reducing the number of events to be transmitted, while at the same time increasing the information content of the remaining events. Considering the telemetry allocation to JEM-X, this means an improved overall performance for the instrument, particularly for observations in the plane of the Galaxy.

The JEM-X imaging is affected by some (limited) coding noise, but does not suffer from "ghost" images because the pattern of the mask only repeats itself near the edges of the mask.

The mask height above the detector (~3.4 m) and the hexagonal mask element dimension (3.3 mm centre-to-centre) define together the angular resolution of the instrument, in this case 3′. Figure 4 illustrates the JEM-X coded mask pattern.

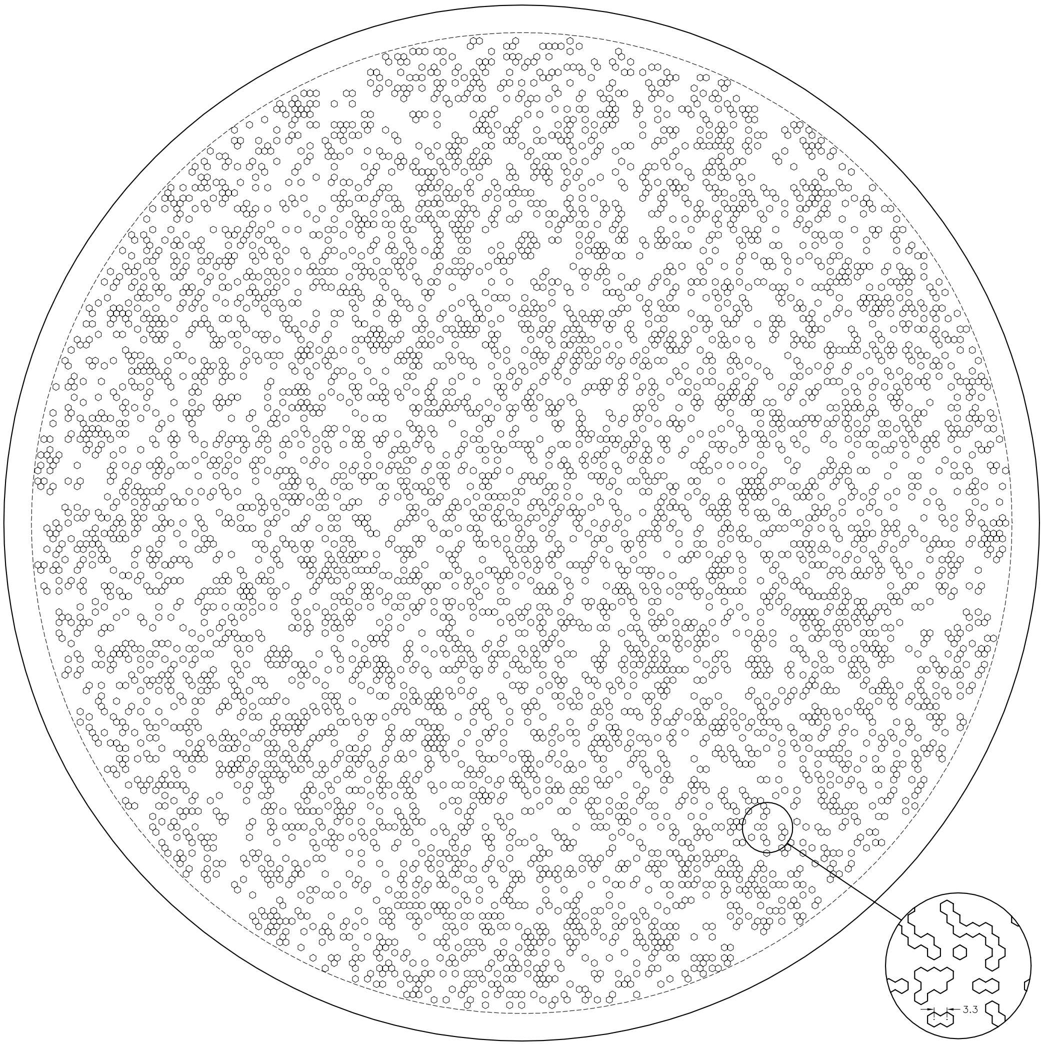

Figure 4: Illustration of the JEM-X coded mask pattern layout without the mechanical interface. The diameter of the coded mask is 535 mm. The mask has a transparency of 25%

3 Instrument operations

3.1 Telemetry formats and their use

A number of telemetry formats have been defined for the JEM-X instruments in order to make the best of a situation with a limited telemetry band-width. Two types of on-board data reduction can take place:

1) a grey filter can randomly remove *some of the events* from the telemetry data stream
2) a "reduced event" telemetry format removes *part of the information* about each event from the telemetry data stream. The telemetry format is selected by the user when preparing a proposal.

The so-called FULL IMAGING event data format is the standard format and is strongly recommended for almost all observation situations. The grey filter mechanism described in the next section works well to make the best use of the available telemetry capacity.

The FULL IMAGING format contains adequate information about event position, time, and energy. All the other formats remove part of that information from each event, thus requiring fewer bytes per event. A detailed description of the various formats is given in section 3 below. For each observation the observer must select a "primary" and a "secondary" format. When the observation starts the primary format (e.g. FULL IMAGING) will be in effect. If the actual count rate is too high for this format the instrument will autonomously switch to the secondary format. For JEM-X count rates higher than about 70 cts/s including background, or ~600 mCrab, the grey filter random event rejection will take place. Alternatively the user may specify a more densely packed "secondary" telemetry format at the cost of information per event. When the count rate exceeds a certain value the instrument will autonomously switch to this mode - and switch back when no longer needed. This, however, complicates the data analysis and experience shows that setting both the primary and the secondary format to FULL IMAGING is the best choice.

The conversion from recorded PHA value to energy depends on where the photons fall on the detector. Hence the non-imaging formats lead to a reduced energy resolution. The detector background is higher at the edge of the detector. The non-imaging formats include these edges that can be avoided in the imaging formats (FULL and RESTRICTED IMAGING). The RESTRICTED IMAGING mode, however, has very limited energy resolution.

The selection is made by the proposer when using the Proposal Generation Tool (PGT, see the **Mission Overview** document).

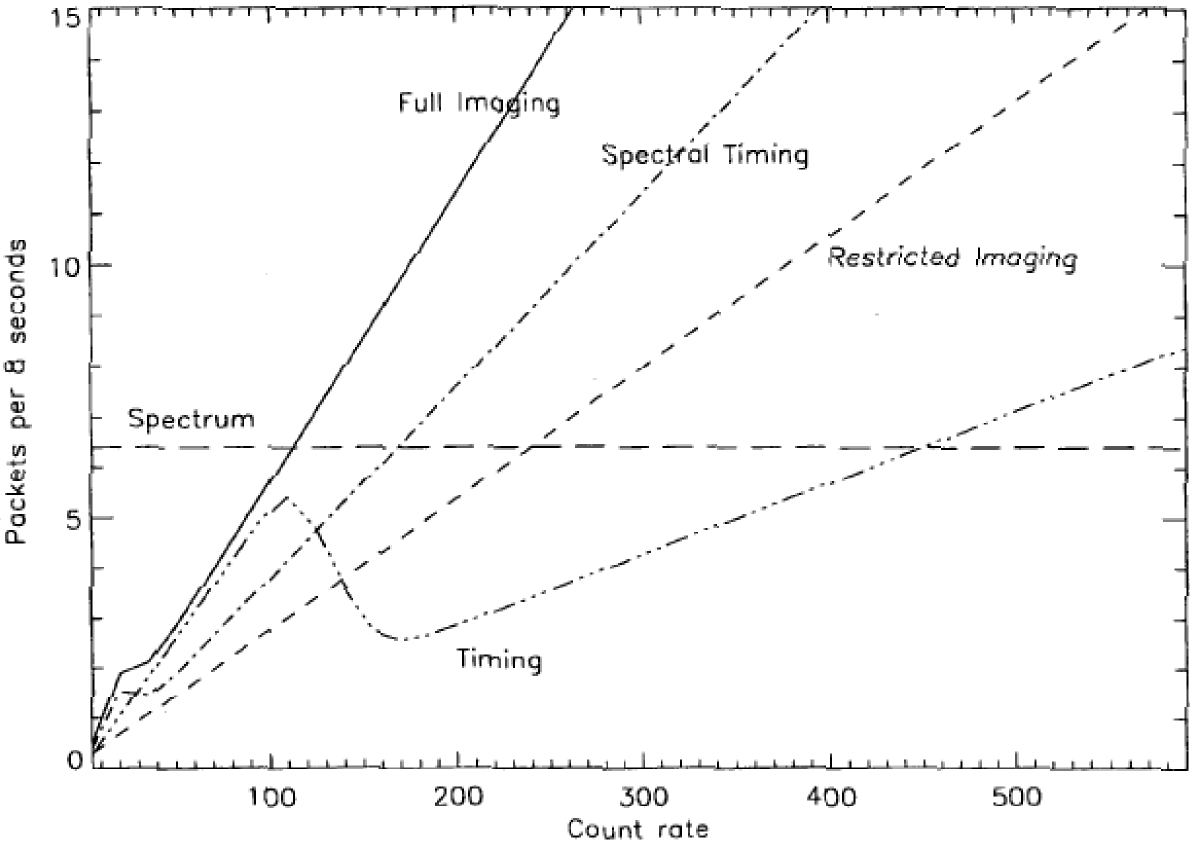

Figure 5: Telemetry rate per JEM-X unit, in packets per cycle of 8 seconds, for the 5 different telemetry modes: Full Imaging, Restricted Imaging, Spectral Timing, Timing and Spectrum. The maximum value for science data transmission, per JEM-X unit is 7/(8 s).

3.2 The grey-filter mechanism

The grey-filter process can operate with 32 different transmission fractions. These fractions are T= 1/32, 2/32, ..., 31/32, 32/32. The filter values to be used will be chosen by the instrument electronics during the actual observation, taking into account the total background count rates. The grey filter will always be adjusted automatically by the on-board software to match the data stream to the available telemetry capacity, thus the term “automatic grey filter”. Whenever the grey filter level is changed (decrease or increase) the on-board software checks whether a telemetry format change should also take place. When the format changes from primary to secondary the value of the grey filter does not change initially. When the format switches back from secondary to primary the grey filter is automatically adjusted.

3.3 Detailed overview of the telemetry formats

The primary and secondary telemetry formats are the only instrumental parameters that need to be set by the general observer through the Proposal Generation software (PGT). Their characteristics are listed in Table 2. *We strongly recommend that for "normal" observations users select* **FULL IMAGING** *for both the primary and the secondary format* for it is the only way to ensure a good measurement of the X-ray background flux. (N.B. The rest of this section gives a detailed overview of the telemetry formats, so most observers can skip it and proceed to the next section).

Figure 5 above shows the behavior of the telemetry rate versus count rate for the five JEM-X telemetry modes.

Table 2: Characteristics of the JEM-X Telemetry Formats.

Format Name	Detector Image Resolution (pixels)	Timing Resolution	Number of Spectral Channels
Full Imaging	256 x 256	1/8192s = 122μs	256
Restricted Imaging	256 x 256	1/8 s = 125 ms	8
Spectral Timing	None	1/8192s = 122μs	256
Timing	None	1/8192s = 122μs	None
Spectrum	None	1/8s = 125 ms	64

Here are some further comments on the use of the telemetry formats (as primary or secondary):

FULL IMAGING: This is the main JEM-X format. It is recommended as primary and secondary format for most "standard" observations. If the count rate does not exceed 200 cts/s, no other formats should be considered. The event positions, pulse heights and arrival times are transmitted.

RESTRICTED IMAGING: This format should only be used as a secondary format (with FULL IMAGING as the primary format) and only in a situation where the purpose is to study a weak source close to a very strong source (> 2 Crab).
This format provides all imaging capabilities of FULL IMAGING, but provides limited spectral resolution (8 channels) and timing resolution (1/8 s).

SPECTRAL TIMING: This format provides timing and spectral capabilities, but *no* imaging. It may useful for observing fields with only one strong source, where imaging may be less important. It should be noted that actual physical spectral resolution is degraded because of the gain variation across the detector.

TIMING: Provides only the timing information of FULL IMAGING. The format is only suited for observations where one strong source dominates the field of view and where the interest is in the timing analysis. *No* position or spectral data is transmitted.

SPECTRUM: This format provides limited spectral resolution (64 channels) with limited time resolution (1/8 s). The format is only suited for observations where one strong source dominates the field of view. It is only to be considered at count rates above approximately 500 cts/s. *No* position data is transmitted.

3.4 Combining primary and secondary telemetry formats

When selecting the primary and the secondary format for a given observation only a restricted set of combinations is meaningful and possible. One essential rule is that the secondary format must not be less efficient in terms of event throughput than the primary format. Another constraint comes from the condition that the two formats to be combined as primary and secondary must have some significant data characteristics in common. For example, it does not make much sense to combine Restricted Imaging, which has only very limited timing and spectral capabilities, with the Spectral Timing, Timing or Spectrum formats. The Spectrum format does not combine with any of the other formats because the corresponding data are handled very differently on-board. These constraints are illustrated in Table 3. In case the same format is selected for primary and secondary, grey filtering will automatically switch in to limit the telemetry if the count rate limit is exceeded.

It should also be noted that, in the case of an amalgamation (see the **Mission Overview document)** of two or more observations, only the primary JEM-X telemetry format of the individual observations will come into consideration for JEM-X compatibility.

Table 3: Possible combinations of primary and secondary telemetry formats.

Secondary Format → **Primary Format↓**	**Full Imaging**	**Restricted Imaging**	**Spectral Timing**	**Timing**	**Spectrum**
Full Imaging	yes	yes	yes	yes	no
Restricted Imaging	no	yes	no	no	no
Spectral Timing	no	no	yes	yes	no
Timing	no	no	no	yes	no
Spectrum	no	no	no	no	yes

3.5 Ranges of usefulness of telemetry formats

Each telemetry format has a certain range of count rates which are optimal for the scientific priorities of an observation. Full Imaging is always optimal with respect to the amount of information about the transmitted events. However, only 70 events/s can be transmitted before the grey-filtering process will begin to reject good events (see Table 9 in section V for examples of real count rates). So, in very specific conditions, e.g. when observing crowded fields near the galactic centre or wanting to study a weak AGN in the vicinity of a bright source, the loss of events may not be acceptable and the Restricted Imaging format may be considered. In other cases, where the timing information is essential the Spectral Timing or pure Timing formats may be preferred despite the total loss of information about eventual background caused by other sources in the field. Table 4 shows the estimated ranges of usefulness of the different telemetry formats.

Table 4: Ranges of usefulness of telemetry formats.

Format name	**Rate of useful events (counts / second)**	**Preferred format with less restrictions**
Full Imaging	70	None
Restricted Imaging	270	Full Imaging
Spectral Timing	180	Full Imaging
Timing	500	Spectral Timing
Spectrum	2000	Spectral Timing

4 Performance of the instrument

JEM-X is currently operated with one active and one dormant unit. The nominal telemetry allocation is 7 science packets and one housekeeping packet per 8 seconds for the active unit. This allows to transmit about 90 counts/s before events will begin to pile up in the onboard buffer – thiswill eventually force the grey filter mechanism to set in. (90 counts/s corresponds to about 500 mCrab source counts plus the solar minimum instrumental background). At the beginning of a new pointing (science window) the grey filter is set to full transmission, and therefore, even for higher count rates there will allways be a period in the beginning of every pointing where all data are transmitted – the catch is that some of the data taken at the end of the pointing may be lost as the on-board buffers are flushed when the following pointing begins.

4.1 Background

The JEM-X background during solar minimum conditions has been measured from a number of empty field observations. The background rate currently is about 30 counts/s in the 3 to 40 keV range, when the spacecraft is outside the radiation belts. Figure 6 shows a background spectrum from JEM-X1, averaged over 60 empty-field observations in March 2004. The background radiation environment is mainly produced by two components: the diffuse X-ray background and the X- and gamma-radiation induced by cosmic rays. The diffuse X-ray background dominates the background below about 15 keV and the cosmic ray induced background dominates at higher energies. The line at about 30 keV is due to fluorescence photons from the Xenon gas in the volumes surrounding the active detector volume. (It is a useful calibration line and an indicator of the effective resolution of the instrument).

There are other instrumental lines visible as well. The background increases noticeably at the edge of the detector which is why the useful detector diameter is only 220 mm, rather than the 250 mm physical diameter. (The useful diameter depends on the chosen energy range because the background is strongly energy dependent). The rejection of background events produced by charged particles crossing the detector is accomplished with a combination of pulse height, pulse shape and "footprint"-evaluation techniques. These techniques reach a particle rejection efficiency better than 99.5%.

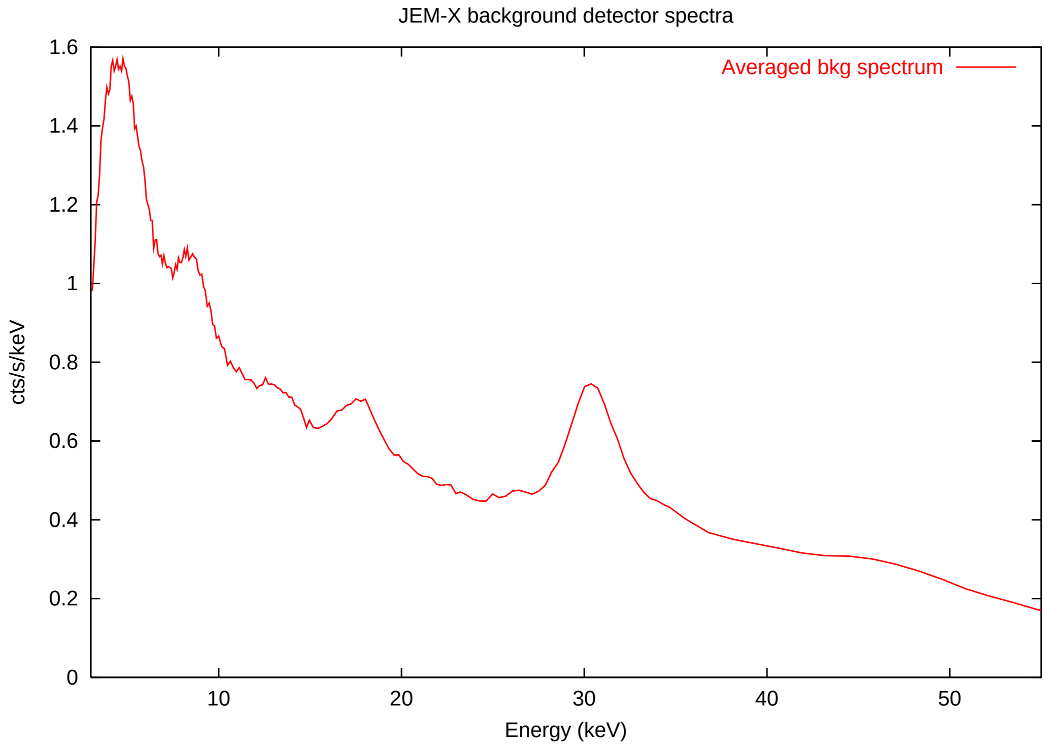

Figure 6: All-detector spectrum of empty field observations showing the combined diffuse and instrumental background.

4.2 Timing stability and resolution

JEM-X observations of the Crab pulsar have shown that the absolute timing is stable to better than 100 µs. The individual JEM-X counts are time binned into bins of width 122 µs. However, the Crab analysis shows, that the phase of the timing bins is stable within a few µs.

4.3 Imaging: resolution and detection limits

The accuracy of source position determinations depends on the number of source and background counts and on off-axis angle of the source. Analysis of the standard JEM-X images show that the point spread function of JEM-X is well represented by a symmetrical 2D Gaussian function with a standard deviation of 1.6 arcminutes. This resolution defines the JEM-X ability to check for the presence of multiple sources and also the ability to separate spectra from two sources at small angular separations.

The source position accuracy depends both on source properties (source spectrum and source strengths) and on instrument characteristics. The important instrument characteristics are: the mask cell size, the intrinsic detector position resolution and the detector alignment with respect to the celestial reference frame.

The source positions are best determined when sources are observed on-axis. The JEM-X vignetting function has the shape of a pyramid, so even within the central "fully illuminated" region the instrument response varies significantly between different off axis positions.

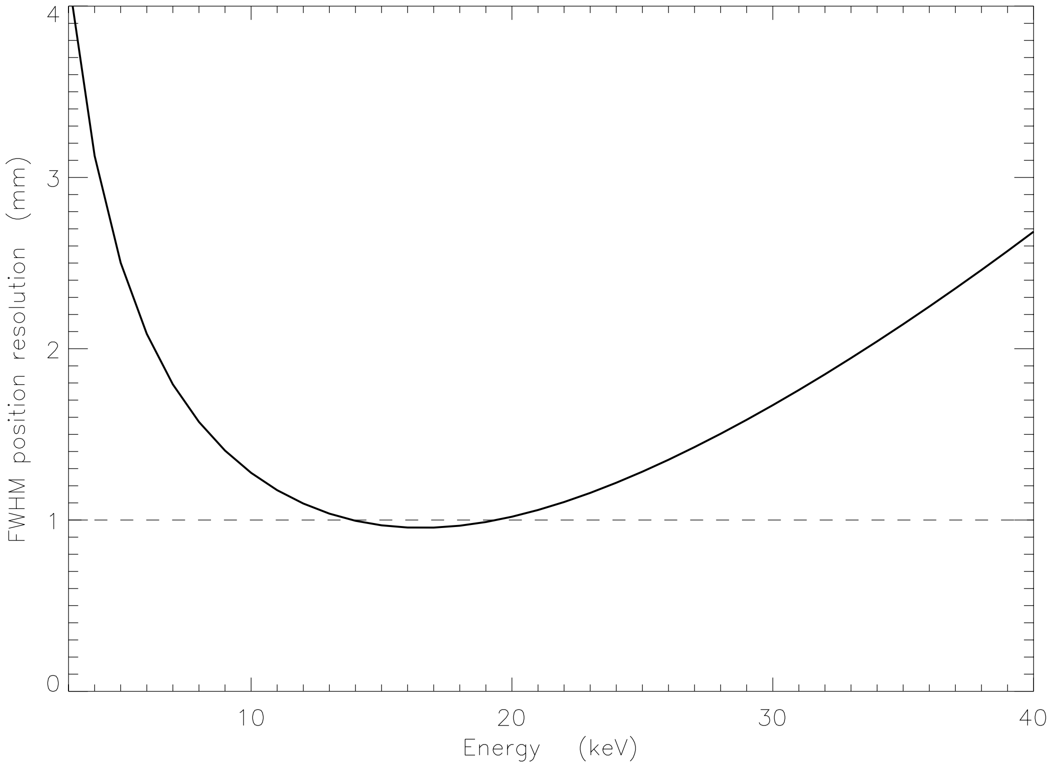

Figure 7: The position resolution in the detector as a function of energy. Note that the positions are rounded to 1mm accuracy in the down-linked data.

The intrinsic detector position resolution is shown as function of energy in Figure 7 for photons entering on-axis. The degradation below 10 keV is caused by the electronic noise of the front-end amplifiers, that above 10 keV by the increase of the primary photo-electron range with energy. The intrinsic position resolution of the detector is finer than the pixel size of the coded mask (3.3 mm) over most of the energy range. The determination of the photon positions in the image plane is affected by parallax for higher energy photons entering at off axis angles. This effect is not of prime importance for source positioning, but the smearing of the image affects the off-axis sensitivity at energies above 20 keV.

The alignment of the detector with respect to the INTEGRAL star trackers appear to be stable to better than 10 arcseconds, and the star tracker accuracy is even better than this. The JEM-X OSA 5.1 software has systematic errors of about 30 arcseconds, and therefore does not reproduce the expected accuracy, but work is underway to reduce these systematics.

The source detection limit for single science windows depends on the background conditions and on the off-axis angle of the source, but 20 mCrab sources are reliably detected under normal background conditions if they appear less than 3 degrees off axis. Better sensitivities can be obtained by “mosaicking” overlapping images from several science windows. See also section 4.5 below.

4.4 Detector energy resolution

The energy resolution of the JEM-X instruments slowly degrades with time when the instruments are used. This is the primary reason why only one JEM-X unit is used at a time. Two effects have been noted to change over time: one is an increase in the recovery time for local modifications (drops) in the gas amplification following large charge deposits on the microstrip plate caused by the passage of heavy cosmic rays. The second effect is a gradual change (increase) of the gas amplification for a constant detector voltage. This change is not the same everywhere on the detector, and requires remapping the gain map using the xenon fluorescense line from time to time. Physically, the degradation is supected to be caused by gradual changes in the conductivity of the microstrip glass substrate due to ion migration. The JEM-X team generates regular updates to the response files to be used with the OSA, in order to respond to this evolution.

The degradation of the energy resolution is most noticeable at the highest energies. It can be described by an additional, slowly time-varying, term in the equation below

$$\Delta E/E = 0.4 \times [(1/E[keV]) + (1/(E_{noise})[keV])]^{1/2}$$

E_{noise} can be interpreted as that energy where the resolution has degraded by a factor sqrt(2). For JEM-X 1, after two years of use, E_{noise} is close to 40 keV.

4.5 Sensitivity (continuum and lines)

Figure 8 andFigure 9 illustrate the source detection capabilities obtained from mosaic images as function of effective accumulated observation time corrected for dead time, grey filter and vignetting effects.

Figure 10 and Figure 11 show the detection limits for narrow lines at 6 keV (close to the Iron K line complex) and at 20 keV as well as the loci for 0.001, 0.1 and 1 keV Equivalent Width (EW).

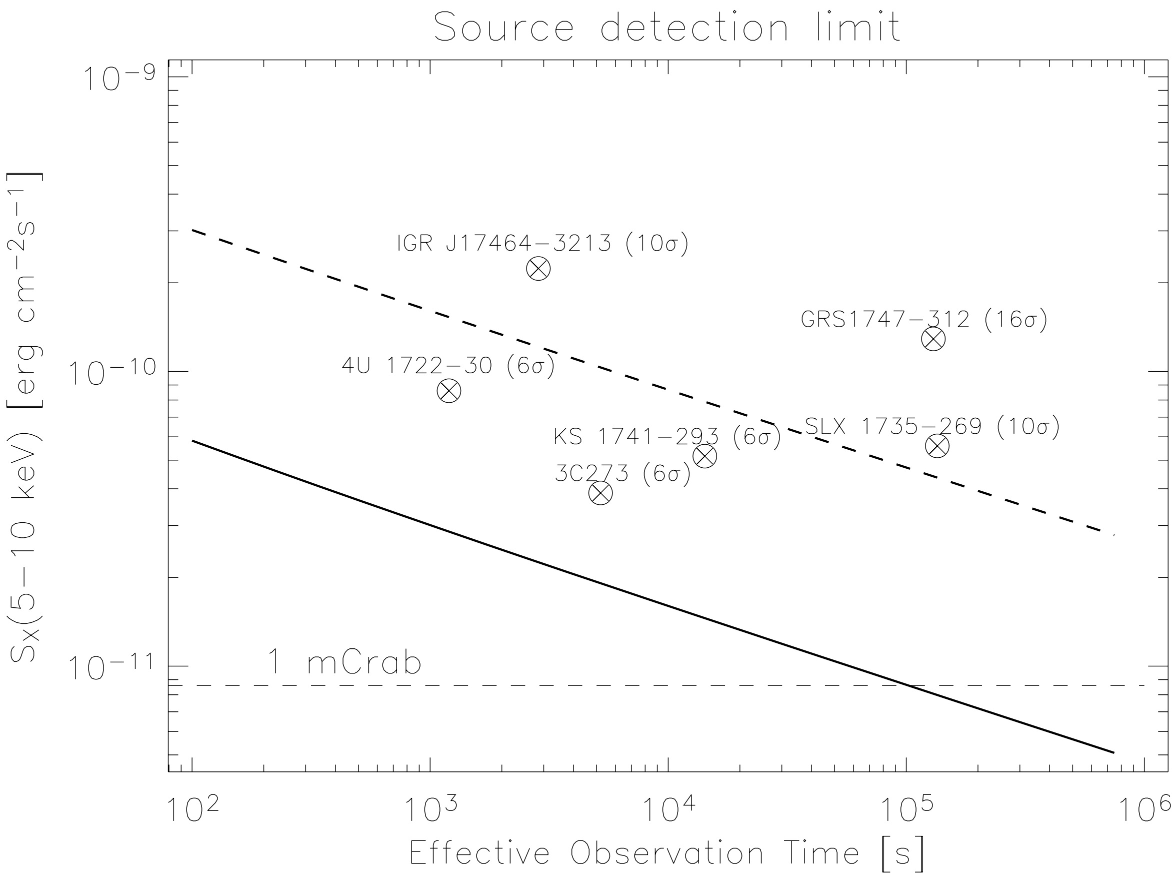

Figure 8: Source detection capabilities in the 5 to 10 keV band as function of effective accumulated observation time in JEM-X mosaic images corrected for dead time, grey filter and vignetting effects. The thick solid curve is obtained from simulations where an isolated source must be detected at 6 σ in the deconvolved image. The dashed line represent the case where there are additional sources in the field of view providing background corresponding to the count rate from the Crab. The source 3C 273 is an example of an isolated source, the other sources comes from observations in the crowded Galactic center region. The σ-values given in parentheses are obtained from mosaic maps with default pixel size (1.5 arcmin)

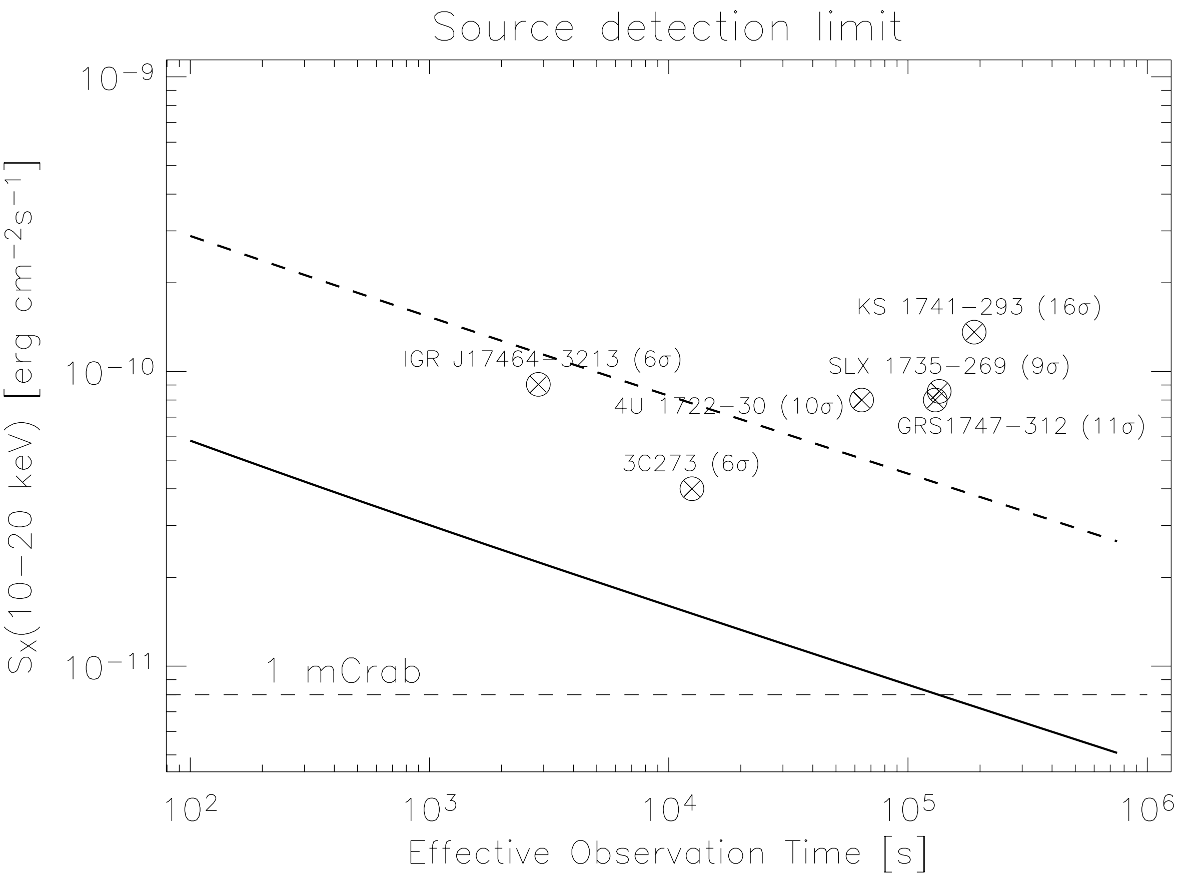

Figure 9: Source detection capabilities in the 10 to 20 keV band as function of effective accumulated observation time in JEM-X mosaic images corrected for dead time, grey filter and vignetting effects. The thick solid curve is obtained from simulations where an isolated source must be detected at 6 σ in the deconvolved image. The dashed line represent the case where there are additional sources in the field of view providing background corresponding to the count rate from the Crab. The source 3C 273 is an example of an isolated source, The other sources comes from observations in the crowded Galactic center region. The σ-values given in parentheses are obtained from mosaic maps with default pixel size (1.5 arcmin).

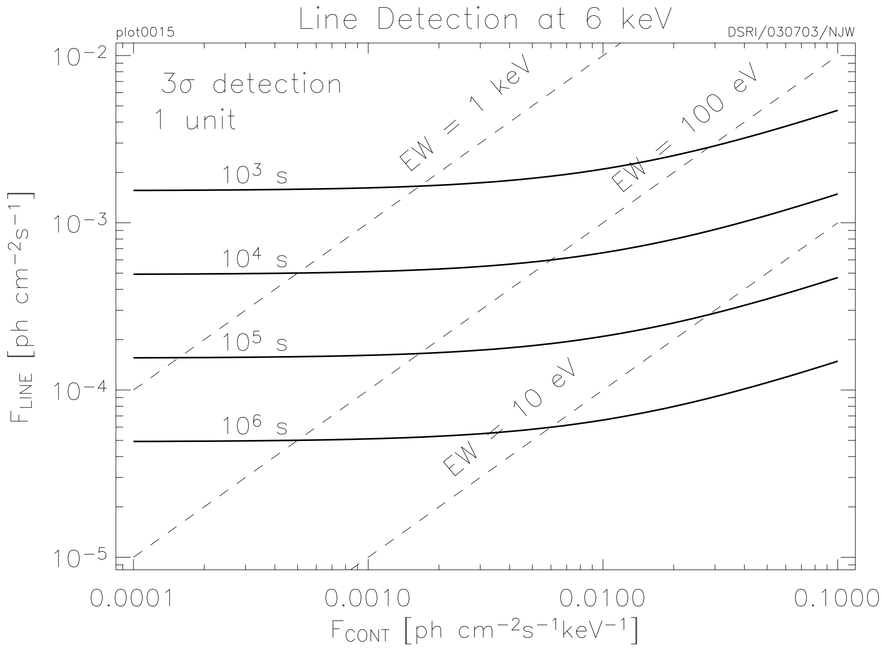

Figure 10: The 3σ line detection limits at 6 keV as a function of the continuum flux at 6 keV, for a single JEM-X unit. The dashed lines represent constant Equivalent Width (EW).

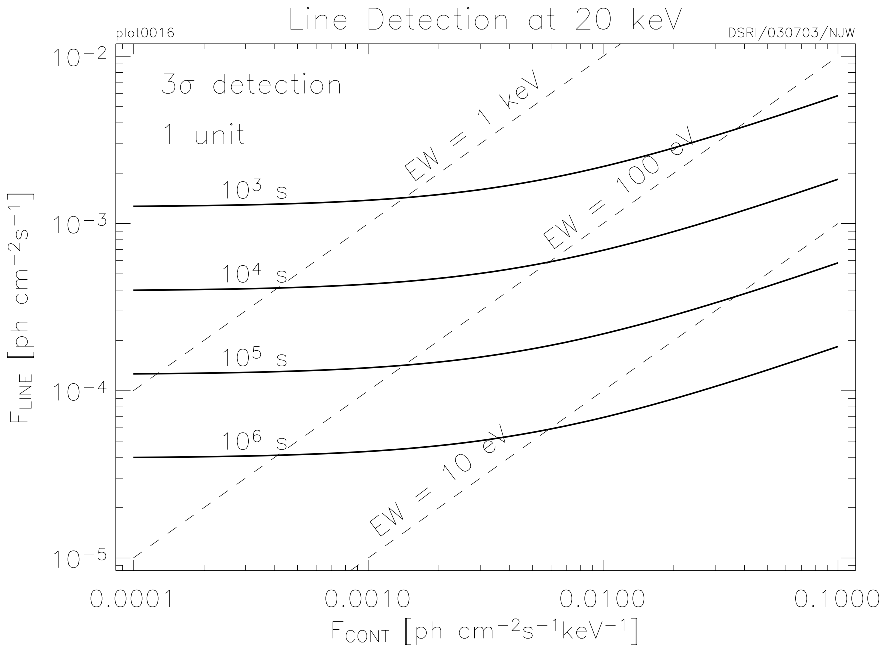

Figure 11: The 3σ line detection limits at 20 keV as a function of the continuum flux at 20 keV, for a single JEM-X unit. The dashed lines represent constant Equivalent Width (EW).

5 Observation "cook book"

5.1 Considerations of the use of the instrument

The primary role of JEM-X is to provide data on the X-ray flux and variability of the targets observed by the two main gamma-ray instruments IBIS and SPI. JEM-X can often pinpoint the source positions with a better precision than IBIS and is thus capable of contributing to the identification of new sources.

The sensitivity of a coded mask instrument like JEM-X is critically dependent on the software used to analyse the data - much more so than for simpler types of X-ray instruments. The sensitivity examples mentioned below should therefore not be considered as final - even after several months of intensive post-launch calibration work there are still several known shortcomings in the analysis software. Improvements in the spectrum extraction software are expected which may increase the S/N. Likewise, specific user choices during the data analysis can reduce the effective area to be used for a given JEM-X data set. This can lead to the necessity of using constant offsets when doing simultaneous spectral fitting of JEM-X spectra together with other Integral spectra.

Users should also be aware that the current spectral extraction and vignetting corrections for sources with off-axis angles greater than 3 or 4 degrees should be interpreted with caution.

Concerning the source detectability, it can be noted that during the Galactic Plane Scan observations (2200 s each) sources down to 20 mCrab are reliably detected when they are inside the central 10° of the field of view. In the same observations many weaker sources -down to 3 mCrab- are also found if they are within the central few degrees of the field of view. These numbers refer to observations with a single JEM-X unit.

5.2 Loss of JEM-X sensitivity due to dithering

Most INTEGRAL observations are done using a 5x5 dither pattern with points spaced 2° apart. Dithering is necessary for SPI and recommended for IBIS. Unfortunately, such dithering does not allow JEM-X to observe the target source continuously. In the 5x5 mode, only the central 9 out of the 25 dither pointings yield useful JEM-X spectral data for the central source. This is due to the fact that the target is off-axis during part of the dither pointings (see also Figure 2). Table 5 shows the average degradation for the different spacecraft dithering patterns.

Table 5: Effective JEM-X observation times for different dithering modes.

Dithering mode	Effective observation time
Staring	100%
Hexagonal dither	69%
''5 × 5'' dither	23% (2.17° step size), 27% (2° step size)

5.3 How to estimate observing times

This section describes how to estimate observing times in order to detect X-ray continuum emission and line emission with JEM-X. It is assumed that there is *no dithering* (i.e. STARING mode) and that only one JEM-X unit is used. The instrument sensitivities quoted here are basically the same as in AO-3.

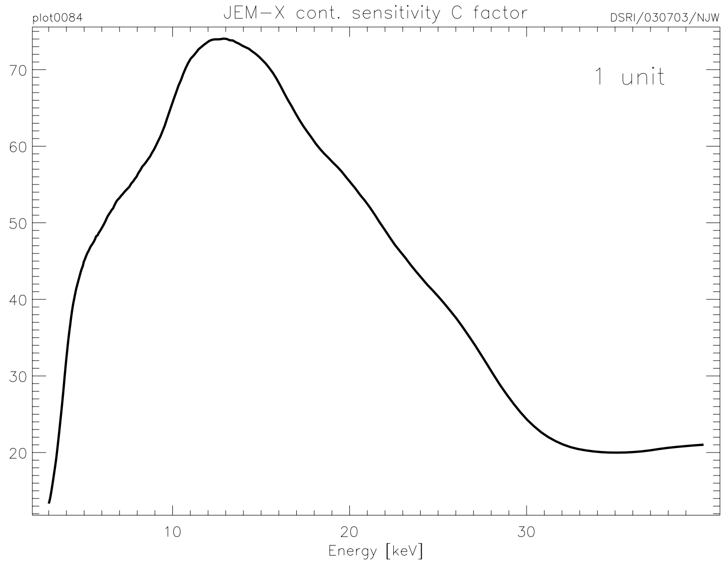

Figure 12: C-factor for estimating the continuum sensitivity, for a single JEM-X unit.

5.4 Continuum emission

Figure 12 gives a plot of the factor *C(E)* to be used together with the following equation in order to estimate the continuum sensitivity for various detection levels (N_σ = number of sigmas) and observation times t_{obs} (s). $F_{cont}(E)$ is the continuum flux (photons cm^{-2} s^{-1} keV^{-1}) and ΔE the energy resolution (keV):

$$N_\sigma = F_{cont}(E) \times \sqrt{\Delta E \times t_{obs}} \times C(E)$$

5.5 Line emission

Figure 13 gives a plot of the factor $L(E, F_{cont})$ to be used together with either of the following equations in order to estimate the line detection sensitivity for various detection levels (N_σ = number of sigmas) and observation times (t_{obs}).

$$N_\sigma = F_{line}(E) \times \sqrt{t_{obs}} \times L(E, F_{cont})$$

$$N_\sigma = F_{cont}(E) \times EW \times \sqrt{t_{obs}} \times L(E, F_{cont})$$

where $F_{line}(E)$ is the line flux (photons cm^{-2} s^{-1}), F_{cont} the source continuum flux at energy E (photons cm^{-2} s^{-1} keV^{-1}), and EW the equivalent width in keV.

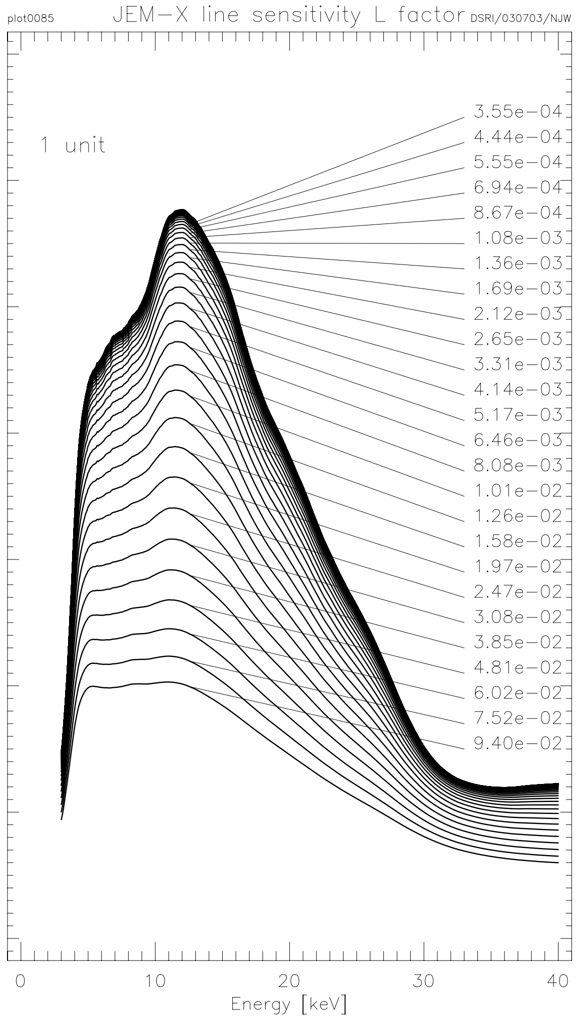

Figure 13: The L-factor for estimating the line detection sensitivity. There is a curve for each value of the continuum flux (indicated in photons / (cm2 s keV)). The L-factor is plotted as a function of the energy of the line feature and is for a single JEM-X unit.

5.6 Practical examples

This section gives some practical examples which illustrate the use the formulae described in section 2. To conclude, Table 9 lists the actual JEM-X background count rates for a single JEM-X unit as well as the observed count rates for the Crab (Nebula+pulsar) on-axis, as measured in-orbit.

5.7 Example #1: spectroscopy and continuum studies

Consider a 10 mCrab AGN with photon spectral index of 1.7. What is the capability of JEM-X for (i) spectroscopy, (ii) broad-band measurements?

Assume a staring observation, i.e. no sensitivity loss due to dithering.

Assume in each case that we want a 5σ measurement within a bandwidth ΔE.

For spectroscopy we choose a ΔE consistent with the spectral resolution at E: ΔE=0.4$\times E^{1/2}$

It is clear from Table 6 that a short (10^5s) observation will not yield a high quality JEM-X spectrum on this source. However, for broad-band studies, choosing $\Delta E = E$, we at least achieve a measurement of the X-ray 'colour', as shown in Table 7.

Table 6: JEM-X spectroscopy

E(keV)	ΔE(keV)	Flux (photons $cm^{-2}s^{-1}keV^{-1}$)	C(E)	Required Observation Time (s)
4	0.8	5.0×10^{-4}	33	1.2×10^{5}
10	1.3	1.0×10^{-4}	67	4.3×10^{5}
20	1.8	3.0×10^{-5}	55	5.1×10^{6}

Table 7: JEM-X broad-band capability

E(keV)	ΔE(keV)	Flux (photons $cm^{-2}s^{-1}keV^{-1}$)	C(E)	Required Observation Time (s)
4	4	5.0×10^{-4}	33	2.3×10^{4}
10	10	1.0×10^{-4}	67	5.6×10^{4}
20	20	3.0×10^{-5}	55	4.6×10^{5}

5.8 Example #2: broad band variability

Consider a bright X-ray binary - 1/3 of the intensity of the Crab. We wish to perform a 'staring' observation of 9×10^4s to measure the variability in two energy bands, 3-10 keV and 10-30 keV. How sensitive are we to rapid variability?

Table 8: N_σ for an exposure of 9×10^4 s

Band (keV)	E (keV)	ΔE (keV)	Flux (photons $cm^{-2}s^{-1}keV^{-1}$)	C(E)	N_σ in $t=9\times10^4$s
3 - 10	6	7	0.09	50	3572
10 - 30	20	20	0.008	55	590

Assume we want a 5σ signal. The required time scales as the square of N_σ (see Table 8), so in the softer band we would achieve a 5σ signal in 0.2s, in the harder band in 6.5s.

5.9 Example #3: broad band variability and dithering

Consider the same source as in Example 2 but using a 5 × 5 dither pattern and performing the full scan just once, in 4.5×10^4s. In addition, we have a 66% loss in sensitivity in this dither pattern compared to the staring observation in Example 2. The value of N_σ scales linearly with the sensitivity and as the square root of the integration time.

In this case (4.5×10^4 s) we achieve:

$N_\sigma = 860 = (1\text{-}0.66) \times 0.09 \times (7 \times 4.5 \times 10^4)^{1/2} \times 50$ at 6 keV and

$N_\sigma = 140 = (1\text{-}0.66) \times 0.008 \times (20 \times 4.5 \times 10^4)^{1/2} \times 55$ at 20 keV.

Times for a 5σ signal are 1.5 s and 57 s, respectively; however at every consecutive dither the effective sensitivity changes and this may introduce artifacts into the light curve on time-scales corresponding to the variable dither patterns.

5.10 Example #4: line detection

Consider a source with a power-law spectrum and spectral photon index = 1.5. It is expected to have a line feature at 20 keV with EW = 0.5 keV. The source strength in the interval 2 - 10 keV is 1.0×10^{-9} erg cm^{-2} s^{-1}.

F_{cont}(20 keV) = 2.0 10^{-3} photons cm^{-2}s^{-1}keV^{-1},

F_{line} (expected) = 1.0 10^{-3} photons cm^{-2}s^{-1},

L(E=20 keV; F_{cont}=2.0 10^{-3} photons cm^{-2}s^{-1}keV^{-1}) = 36 (read from curve in Fig. 13),

$t_{obs} = 4 \times 10^4$ s implies a detection level: $N_\sigma = 0.001 \times 200 \times 36 = 7.2$,

which is a good detection.

5.11 Example #5: in-orbit count rates for the Crab and the JEM-X background

Table 9: Count rates for a single JEM-X unit (Crab on-axis).

Interval [keV]	**Crab counts s^{-1}**	**Diffuse X-ray Background counts s^{-1}**	**Cosmic Ray induced counts s^{-1}**	**Total bkg counts s^{-1}**
3 - 10	83	3	3.1	6.1
10 - 20	27	1.8	5.1	6.9
20 - 35	5.4	0.5	6.5	7.0
Total: 3 - 35	115	5.3	14.7	20.0